J|A|C|S ARTICLES

Published on Web 04/06/2010

Efficient Nonsacrificial Water Splitting through Two-Step Photoexcitation by Visible Light using a Modified Oxynitride as a Hydrogen Evolution Photocatalyst

Kazuhiko Maeda,[†] Masanobu Higashi,[‡] Daling Lu,[§] Ryu Abe,[‡] and Kazunari Domen*[,†]

Department of Chemical System Engineering, The University of Tokyo, 7-3-1 Hongo, Bunkyo-ku, Tokyo 113-8656, Japan, Catalysis Research Center, Hokkaido University, Sapporo 001-0021, Japan, and Center for Advanced Materials Analysis, Tokyo Institute of Technology, 2-12-1 Ookayama, Meguro-ku, Tokyo 152-8550, Japan

Received February 1, 2010; E-mail: domen@chemsys.t.u-tokyo.ac.jp

Abstract: A two-step photocatalytic water splitting (Z-scheme) system consisting of a modified ZrO_2/TaON species (H_2 evolution photocatalyst), an O_2 evolution photocatalyst, and a reversible donor/acceptor pair (i.e., redox mediator) was investigated. Among the O_2 evolution photocatalysts and redox mediators examined, Pt-loaded WO_3 (Pt/WO_3) and the IO_3^-/I^- pair were respectively found to be the most active components. Combining these two components with Pt-loaded ZrO_2/TaON achieved stoichiometric water splitting into H_2 and O_2 under visible light, achieving an apparent quantum yield of 6.3% under irradiation by 420.5 nm monochromatic light under optimal conditions, 6 times greater than the yield achieved using a TaON analogue. To the best of our knowledge, this is the highest reported value to date for a nonsacrificial visible-light-driven water splitting system. The high activity of this system is due to the efficient reaction of electron donors (I^- ions) and acceptors (IO_3^- ions) on the Pt/ZrO_2/TaON and Pt/WO_3 photocatalysts, respectively, which suppresses undesirable reverse reactions involving the redox couple that would otherwise occur on the photocatalysts. Photoluminescence and photoelectrochemical measurements indicated that the high activity of this Z-scheme system results from the moderated n-type semiconducting character of ZrO_2/TaON, which results in a lower probability of undesirable electron−hole recombination in ZrO_2/TaON than in TaON.

1. Introduction

Large-scale hydrogen production from water using a semiconductor photocatalyst with solar energy can potentially produce clean fuel from renewable resources.[1,2] To date, more than 100 photocatalytic systems based on metal oxides have been reported to be active for overall water splitting. Some of these oxides, consisting of early-transition-metal ions (e.g., Ti^{4+}, Nb^{5+}, and Ta^{5+}) modified by a reaction promoter such as NiO, exhibit excellent quantum yields (AQYs), as high as several tens of percent, without the need for sacrificial electron donors or acceptors.[2,3] However, the large band gaps of these metal oxides restrict the utilization of visible photons, which are the main component of the solar spectrum.[4] Therefore, a current research objective in this field is to develop a stable visible-light-responsive photocatalyst capable of achieving overall water splitting, focusing on improved preparation methods and new materials.[2b]

In recent years, extensive studies of individual H_2 and O_2 evolution systems have been performed separately, in an attempt to improve the activities and to obtain mechanistic insight.[5−12]

[†] The University of Tokyo.
[‡] Hokkaido University.
[§] Tokyo Institute of Technology.

(1) Bard, A. J.; Fox, M. A. *Acc. Chem. Res.* **1995**, *28*, 141.
(2) (a) Lee, J. S. *Catal. Surv. Asia* **2005**, *9*, 217. (b) Maeda, K.; Domen, K. *J. Phys. Chem. C* **2007**, *111*, 7851. (c) Osterloh, F. E. *Chem. Mater.* **2008**, *20*, 35. (d) Kudo, A.; Miseki, Y. *Chem. Soc. Rev.* **2009**, *38*, 253.
(3) (a) Ikeda, S.; Hara, M.; Kondo, J. N.; Domen, K.; Takahashi, H.; Okubo, T.; Kakihana, M. *J. Mater. Res.* **1998**, *13*, 852. (b) Kim, H. G.; Hwang, D. W.; Kim, J.; Kim, Y. G.; Lee, J. S. *Chem. Commun.* **1999**, 1077. (c) Kato, H.; Asakura, K.; Kudo, A. *J. Am. Chem. Soc.* **2003**, *125*, 3082. (d) Miseki, Y.; Kato, H.; Kudo, A. *Energy Environ. Sci.* **2009**, *2*, 306.
(4) Scaife, D. E. *Solar Energy* **1980**, *25*, 41.
(5) (a) Abe, R.; Hara, K.; Sayama, K.; Domen, K.; Arakawa, H. *J. Photochem. Photobiol. A: Chem.* **2000**, *137*, 63. (b) Bae, E.; Choi, W. *J. Phys. Chem. B* **2006**, *110*, 14792. (c) Li, Q.; Jin, Z.; Peng, Z.; Li, Y.; Li, S.; Lu, G. *J. Phys. Chem. C* **2007**, *111*, 8237. (d) Li, Q.; Chen, L.; Lu, G. *J. Phys. Chem. C* **2007**, *111*, 11494. (e) Maeda, K.; Eguchi, M.; Lee, S.-H. A.; Youngblood, W. J.; Hata, H.; Mallouk, T. E. *J. Phys. Chem. C* **2009**, *113*, 7962.
(6) (a) Tsuji, I.; Kato, H.; Kobayashi, H.; Kudo, A. *J. Am. Chem. Soc.* **2004**, *126*, 13406. (b) Tsuji, I.; Kato, H.; Kudo, A. *Angew. Chem., Int. Ed.* **2005**, *44*, 3565. (c) Bao, N.; Shen, L.; Takata, T.; Domen, K. *Chem. Mater.* **2008**, *20*, 110. (d) Yan, H.; Yang, J.; Ma, G.; Wu, G.; Zong, X.; Lei, Z.; Shi, J.; Li, C. *J. Catal.* **2009**, *266*, 165.
(7) (a) Hara, M.; Mallouk, T. E. *Chem. Commun.* **2000**, 1903. (b) Hara, M.; Waraksa, C. C.; Lean, J. T.; Lewis, B. A.; Mallouk, T. E. *J. Phys. Chem. A* **2000**, *104*, 5275.
(8) Jiao, F.; Frei, H. *Angew. Chem., Int. Ed.* **2009**, *48*, 1841.
(9) Silva, C. G.; Bouizi, Y.; Fornés, V.; García, H. *J. Am. Chem. Soc.* **2009**, *131*, 13833.
(10) (a) Hitoki, G.; Takata, T.; Kondo, J. N.; Hara, M.; Kobayashi, H.; Domen, K. *Chem. Commun.* **2002**, 1698. (b) Hitoki, G.; Ishikawa, A.; Takata, T.; Kondo, J. N.; Hara, M.; Domen, K. *Chem. Lett.* **2002**, *31*, 736.

 10.1021/ja1009025

Scheme 1. Schematic Energy Diagrams of Photocatalytic Water Splitting for One-Step and Two-Step Photoexcitation Systems

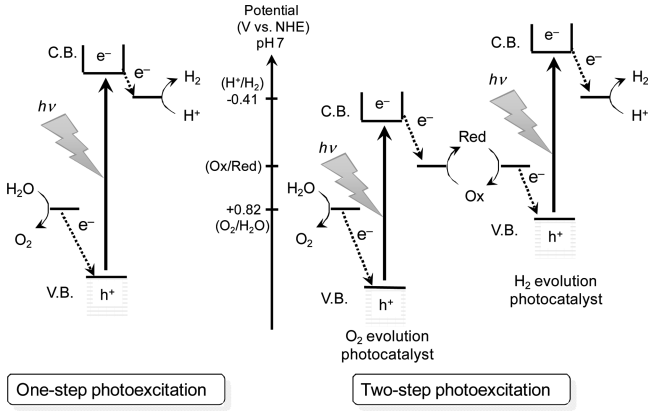

Because of these efforts, high quantum yields as high as several tens of percent can be achieved for these half-reactions, if proper sacrificial electron donors or acceptors are used.[5−11] Although the O_2 evolution reaction is challenging because it involves a multielectron transfer process,[7−11] the combination of H_2 and O_2 evolution systems to decompose water under visible light in a "nonsacrificial" manner remains a significant challenge. Therefore, only a limited number of photocatalytic systems are available for nonsacrificial water splitting under visible light with reasonable reproducibility.

As illustrated in Scheme 1, the successful systems can be primarily divided into two approaches. One approach is to split water into H_2 and O_2 using a single visible-light-responsive photocatalyst with a sufficient potential to achieve overall water splitting.[13,14] The other approach is to apply a two-step excitation mechanism using two different photocatalysts.[15−17] The latter system was inspired by natural photosynthesis in green plants and is called the "Z-scheme". The advantages of a Z-scheme water splitting system are that a wider range of visible light is available because the energy required to drive each photocatalyst can be reduced and that the separation of evolved H_2 and O_2 is possible in principle. It is also possible to use a semiconductor having either a water reduction or oxidation potential for one side of this system. Z-scheme water splitting was introduced by Bard in 1979.[18] Since then, many efforts have been made to construct such systems, focusing on the development of both new materials and effective electron relays.[15−17,19−30] While the number of materials that can be used as H_2 or O_2 evolution photocatalysts in a Z-scheme has increased, the currently available systems remain inefficient.

Our group has attempted to apply (oxy)nitrides to such water splitting systems instead of conventional metal oxide materials, because metal−nitrogen bonding in oxynitrides has a higher potential energy than metal−oxygen bonding in metal oxides, resulting in narrower band gaps (<3 eV).[2b,26−28] According to individual H_2 and O_2 evolution test reactions with the use of proper sacrificial electron donors and acceptors, most (oxy)nitrides exhibit good O_2 evolution activity, while H_2 evolution is a relatively slow process.[2b] Although the ability of (oxy)nitrides to utilize a wide range of visible light (~700 nm) and their photocorrosion resistance motivate their use as a photocatalyst, the use of (oxy)nitrides as a H_2 evolution photocatalyst may seem inefficient.

In this paper, we demonstrate an exceptional result that a modified oxynitride powder, ZrO_2/TaON composite, functions efficiently as an H_2 evolution component of a "nonsacrificial" two-step water splitting system under monochromatic visible light irradiation, with AQYs higher than 6% at 420.5 nm. We previously reported the preparation and characterization of ZrO_2/TaON composite photocatalysts, and the feasibility of this material for photocatalytic H_2 evolution was briefly described.[31] We report here the detailed study of this material as a building block for H_2 evolution in two-step water splitting systems. The reason for the high activity is discussed on the basis of photocatalytic reaction results and photoelectrochemical measurements, and a new concept for an efficient photocatalyst is described.

2. Experimental Section

2.1. Materials and Reagents. ZrO_2/TaON (Zr/Ta = 0.1 by mole) photocatalyst for H_2 evolution was prepared according to a

(11) (a) Kim, H. G.; Hwang, D. W.; Lee, J. S. *J. Am. Chem. Soc.* **2004**, *126*, 8912. (b) Kim, H. G.; Borse, P. H.; Choi, W.; Lee, J. S. *Angew. Chem., Int. Ed.* **2005**, *44*, 4585.
(12) (a) Wang, X.; Maeda, K.; Thomas, A.; Takanabe, K.; Xin, G.; Carlsson, J. M.; Domen, K.; Antonietti, M. *Nat. Mater.* **2009**, *8*, 76. (b) Wang, X.; Maeda, K.; Chen, X.; Takanabe, K.; Domen, K.; Hou, Y.; Fu, X.; Antonietti, M. *J. Am. Chem. Soc.* **2009**, *131*, 1680. (c) Maeda, K.; Wang, X.; Nishihara, Y.; Lu, D.; Antonietti, M.; Domen, K. *J. Phys. Chem. C* **2009**, *113*, 4940.
(13) (a) Maeda, K.; Takata, T.; Hara, M.; Saito, N.; Inoue, Y.; Kobayashi, H.; Domen, K. *J. Am. Chem. Soc.* **2005**, *127*, 8286. (b) Teramura, K.; Maeda, K.; Saito, T.; Takata, T.; Saito, N.; Inoue, Y.; Domen, K. *J. Phys. Chem. B* **2005**, *109*, 21915. (c) Maeda, K.; Teramura, K.; Lu, D.; Takata, T.; Saito, N.; Inoue, Y.; Domen, K. *Nature* **2006**, *440*, 295. (d) Maeda, K.; Teramura, K.; Domen, K. *J. Catal.* **2008**, *254*, 198. (e) Hisatomi, T.; Maeda, K.; Takanabe, K.; Kubota, J.; Domen, K. *J. Phys. Chem. C* **2009**, *113*, 21458.
(14) (a) Lee, Y.; Terashima, H.; Shimodaira, Y.; Teramura, K.; Hara, M.; Kobayashi, H.; Domen, K.; Yashima, M. *J. Phys. Chem. C* **2007**, *111*, 1042. (b) Lee, Y.; Teramura, K.; Hara, M.; Domen, K. *Chem. Mater.* **2007**, *19*, 2120. (c) Takanabe, K.; Uzawa, T.; Wang, X.; Maeda, K.; Katayama, M.; Kubota, J.; Kudo, A.; Domen, K. *Dalton Trans.* **2009**, 10055.
(15) Abe, R.; Sayama, K.; Sugihara, H. *J. Phys. Chem. B* **2005**, *109*, 16052.
(16) Kato, H.; Hori, M.; Konta, R.; Shimodaira, Y.; Kudo, A. *Chem. Lett.* **2004**, *33*, 1348.
(17) Sasaki, Y.; Nemoto, H.; Saito, K.; Kudo, A. *J. Phys. Chem. C* **2009**, *113*, 17536.
(18) Bard, A. J. *J. Photochem.* **1979**, *10*, 59.
(19) Tennakone, K.; Wickramanayake, S. *J. Chem. Soc., Faraday Trans. 2* **1986**, *82*, 1475.
(20) (a) Sayama, K.; Yoshida, R.; Kusama, H.; Okabe, K.; Abe, Y.; Arakawa, H. *Chem. Phys. Lett.* **1997**, *277*, 387. (b) Bamwenda, G. R.; Sayama, K.; Arakawa, H. *J. Photochem. Photobiol. A: Chem.* **1999**, *122*, 175.
(21) Fujihara, K.; Ohno, T.; Matsumura, M. *J. Chem. Soc., Faraday Trans.* **1998**, *94*, 3705.
(22) Abe, R.; Sayama, K.; Domen, K.; Arakawa, H. *Chem. Phys. Lett.* **2001**, *344*, 339.
(23) Sayama, K.; Abe, R.; Arakawa, H.; Sugihara, H. *Catal. Commun.* **2006**, *7*, 96.
(24) (a) Sayama, K.; Mukasa, K.; Abe, R.; Abe, Y.; Arakawa, H. *Chem. Commun.* **2001**, 2416. (b) Sayama, K.; Mukasa, K.; Abe, R.; Abe, Y.; Arakawa, H. *J. Photochem. Photobiol. A: Chem.* **2002**, *148*, 71.
(25) Kato, H.; Sasaki, Y.; Iwase, A.; Kudo, A. *Bull. Chem. Soc. Jpn.* **2007**, *80*, 2457.
(26) Abe, R.; Takata, T.; Sugihara, H.; Domen, K. *Chem. Commun.* **2005**, 3829.
(27) (a) Higashi, M.; Abe, R.; Teramura, K.; Takata, T.; Ohtani, B.; Domen, K. *Chem. Phys. Lett.* **2008**, *452*, 120. (b) Higashi, M.; Abe, R.; Takata, T.; Domen, K. *Chem. Mater.* **2009**, *21*, 1543.
(28) Higashi, M.; Abe, R.; Ishikawa, A.; Takata, T.; Ohtani, B.; Domen, K. *Chem. Lett.* **2008**, *37*, 138.
(29) Sasaki, Y.; Iwase, A.; Kato, H.; Kudo, A. *J. Catal.* **2008**, *259*, 133.
(30) Wang, X.; Liu, G.; Chen, Z.-G.; Li, F.; Wang, L.; Lu, G. Q.; Cheng, H.-M. *Chem. Commun.* **2009**, 3452.
(31) Maeda, K.; Terashima, H.; Kase, K.; Higashi, M.; Tabata, M.; Domen, K. *Bull. Chem. Soc. Jpn.* **2008**, *81*, 927.

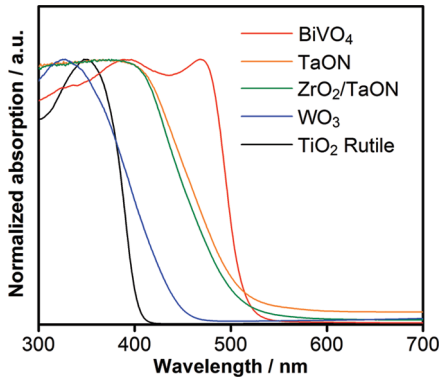

Figure 1. Diffuse reflectance spectra of the particulate photocatalysts used in this study.

method reported previously.[31] WO_3 (High Purity Chemicals, 99.99%), TiO_2 rutile (Kanto Chemicals, 99.0%), TaON, and $BiVO_4$ were employed as O_2 evolution photocatalysts for two-step water splitting. TaON and $BiVO_4$ were prepared according to previous methods.[10a,32] Figure 1 shows UV−visible diffuse reflectance spectra of these samples.

$RuCl_3 \cdot nH_2O$ (Kanto Chemicals, 99.9%), $(NH_4)_2RuCl_6$ (Aldrich), $RhCl_3 \cdot xH_2O$ (Aldrich, 38−40% Rh), $(NH_4)_2PdCl_4$ (Kanto Chemicals, 37% Pd), $Na_2IrCl_6 \cdot 6H_2O$ (Kanto Chemicals, 97% Ir), $H_2PtCl_6 \cdot 2H_2O$ (Kanto Chemicals, 97% Pt), and $HAuCl_4 \cdot 4H_2O$ (Kanto Chemicals, 99.0%) were used as cocatalyst precursors for ZrO_2/TaON and some O_2 evolution photocatalysts. NaI (Kanto Chemicals, reagent grade), $NaIO_3$ (Kanto Chemicals, reagent grade), $FeCl_2 \cdot 4H_2O$ (Wako Pure Chemicals, 99.0−102.0%), and $FeCl_3 \cdot 6H_2O$ (Wako Pure Chemicals, 99.0%) were employed as redox reagents. All chemicals were used without further purification.

2.2. Modification with Cocatalysts. Modification of ZrO_2/TaON with nanoparticulate metal cocatalysts was accomplished by impregnation or in situ photodeposition to improve the water reduction activity.[33] In the impregnation method, ZrO_2/TaON powder was immersed in an aqueous solution containing various amounts of metal precursor in a water bath. After the solution was dried, the resulting powder was collected and heated with H_2 gas (20 kPa) at 473 K for 1 h in a gas circulation system similar to the photocatalytic reaction system described below. Photodeposition was carried out in a glass closed gas circulation system. The powder was immersed in aqueous methanol solution (80 vol%) containing a metal source. The solution was evacuated to remove dissolved air completely and then irradiated with visible light for 5 h. After filtration and washing with pure water, the resulting powder was dried in an oven at 343 K for 24 h.

For WO_3 and TaON, Pt and RuO_2 were respectively loaded as reaction promoters for O_2 evolution, as in previous reports.[15,28] Pt (0.5 wt %)-loaded WO_3 was prepared by immersing WO_3 in aqueous H_2PtCl_6 solution, followed by calcination in air at 823 K for 0.5 h. RuO_2 (0.5 wt %)-loaded TaON was prepared in a similar manner, using $(NH_4)_2RuCl_6$ as the precursor, followed by calcination in air at 623 K for 1 h.

2.3. Characterization of Catalysts. The prepared samples were studied by powder X-ray diffraction (XRD; RINT-UltimaIII, Rigaku; Cu Kα), UV−visible diffuse reflectance spectroscopy (DRS; V-560, JASCO), X-ray photoelectron spectroscopy (XPS; JPS-9000, JEOL), scanning electron microscopy (SEM; S-4700, Hitachi), high-resolution transmission electron microscopy (HR-TEM; JEM-2010F, JEOL), and photoluminescence spectroscopy (PL; FP-6600, Jasco). The binding energies determined by XPS were corrected by reference to the C 1s peak (284.6 eV) for each sample. The PL spectra were measured at liquid nitrogen temperature under excitation at 420 nm provided by emission from a xenon lamp.

2.4. Photocatalytic Reactions. Reactions were carried out in a Pyrex top-irradiation reaction vessel connected to a glass closed gas circulation system whose schematic illustration is displayed in Figure S1 (Supporting Information). Metal-loaded ZrO_2/TaON as an H_2 evolution photocatalyst (50 mg) and an O_2 evolution photocatalyst (100 mg) were suspended using a magnetic stirrer in aqueous solutions (100 mL) containing different concentrations of NaI. The pHs of the solutions were controlled by adding aqueous H_2SO_4 or NaOH if necessary. The reactant solutions were evacuated several times to completely remove any air prior to irradiation under a 300 W xenon lamp. The irradiation wavelength was controlled by a combination of a cold mirror (CM-1) and a water filter ($350 < \lambda < 800$ nm). For visible light irradiation, a cutoff filter (L42) was fitted to the aforementioned light source ($420 < \lambda < 800$ nm). To examine the dependence of wavelength on activity, another cutoff filter was fitted in addition to the L42 filter. The reactant solution was maintained at room temperature by a flow of cooling water during the reaction. The evolved gases were analyzed by gas chromatography. The products were analyzed in the liquid phase by ion chromatography (CO-2060 Plus, Jasco) using Na_2CO_3 aqueous solution (3.6 mM) as the mobile phase.

The apparent quantum yield (AQY) for two-step water splitting was measured using the same experimental setup, except for the addition of a band-pass filter ($\lambda = 420.5$ nm), and was estimated as

$$\mathrm{AQY}(\%) = (A \times R/I) \times 100 \qquad (1)$$

where A, R, and I represent coefficients based on the reactions (H_2 evolution, 4; O_2 evolution, 8), the H_2 or O_2 evolution rate, and the rate of incident photons, respectively.[15−17,24,29] The total number of incident photons (ca. 38.1 mW) was measured using a calibrated silicon photodiode.

3. Results and Discussion

3.1. Effect of Modification of ZrO_2/TaON with Metal Cocatalysts on Water Splitting Activity. First, we tested unmodified ZrO_2/TaON powder as an H_2 evolution photocatalyst from aqueous solutions containing reversible electron donors (e.g., I^- or Fe^{2+}). However, no reaction took place, even under UV and visible light irradiation ($350 < \lambda < 800$ nm). This result inspired us to modify ZrO_2/TaON with metal nanoparticles, which can collect photogenerated electrons from ZrO_2/TaON and act as H_2 evolution sites,[12c,29,34] in an attempt to improve the water reduction behavior. With this modification, ZrO_2/TaON became active for H_2 evolution, enabling its application in two-step water splitting systems. It should be stressed that, under irradiation of light with wavelengths longer than 350 nm, the TaON component in ZrO_2/TaON offers active sites for photocatalytic reactions, while the ZrO_2 modifier does not, because of its large band gap (ca. 5 eV).[31,35]

Table 1 lists the rates of H_2 and O_2 evolution from aqueous NaI solution containing Pt/WO_3 and ZrO_2/TaON modified with various metal cocatalysts (1.0 wt % each), which were loaded by an impregnation method (entries 1−7). Although both ZrO_2/TaON and WO_3 have absorption bands near 500 and 450 nm, respectively (Figure 1), the reactions were conducted under

(32) Iwase, A.; Kato, H.; Kudo, A. Abstract of the Catalysis Society of Japan Fall Meeting, Toyama, Japan, September 26, 2006; p 27.
(33) Kraeutler, B.; Bard, A. J. *J. Am. Chem. Soc.* **1978**, *100*, 4317.
(34) (a) Kamat, P. V. *J. Phys. Chem. B* **2002**, *106*, 7729. (b) Subramanian, V.; Wolf, E.; Kamat, P. V. *J. Phys. Chem. B* **2001**, *105*, 11439. (c) Subramanian, V.; Wolf, E.; Kamat, P. V. *J. Am. Chem. Soc.* **2004**, *126*, 4943.
(35) Sayama, K.; Arakawa, H. *J. Photochem. Photobiol. A: Chem.* **1994**, *77*, 243.

Table 1. Effect of Modification of ZrO_2/TaON with Various Metal Cocatalysts on the Rates of H_2 and O_2 Evolution in Z-Scheme Water Splitting in Combination with Pt/WO_3 and IO_3^-/I^- Shuttle Redox Mediator[a]

entry	cocatalyst (loading/wt %)	loading method	activity[b]/μmol h^{-1} H_2	O_2	H_2/O_2 ratio
1	none		<0.2	0	
2	Ru (1.0)	impregnation	9.8	4.2	2.33
3	Rh (1.0)	impregnation	8.5	2.6	3.27
4	Pd (1.0)	impregnation	3.3	1.0	3.30
5	Ir (1.0)	impregnation	28.4	12.1	2.35
6	Pt (1.0)	impregnation	52.1	26.7	1.95
7	Au (1.0)	impregnation	2.3	trace	
8	Pt (1.0)	photodeposition	6.0	2.0	3.00
9	Pt (0.1)	impregnation	6.1	2.3	2.62
10	Pt (0.5)	impregnation	41.3	21.4	1.93
11	Pt (2.0)	impregnation	25.2	12.1	2.09
12	Pt (3.0)	impregnation	25.1	12.4	2.03

[a] Reaction conditions: catalyst, 100 mg of Pt/WO_3 and 50 mg of Pt/ZrO_2/TaON; aqueous NaI solution, 100 mL (1.0 mM); light source, xenon lamp (300 W) fitted with a cold mirror (CM-1); reaction vessel, Pyrex top-irradiation type; irradiation wavelength, $350 < \lambda < 800$ nm. [b] Average rates of gas evolution in 5 h.

ultraviolet (UV) and visible irradiation ($350 < \lambda < 800$ nm) to utilize more photons in order to obtain more products. As with the hydrogen half-reactions, no appreciable gas evolution was observed when unmodified ZrO_2/TaON was used. Modification of ZrO_2/TaON with metal cocatalysts, however, resulted in simultaneous H_2 and O_2 evolution, indicating that the water-splitting reaction occurred. The water-splitting reaction was initiated by photooxidation of I^- into IO_3^- and photoreduction of H^+ into H_2 on Pt-loaded ZrO_2/TaON catalyst, after which photoreduction of IO_3^- into I^- and photooxidation of H_2O into O_2 occurred on Pt-loaded WO_3 catalyst as follows:

$$I^- + 6h^+ + 6OH^- \rightarrow IO_3^- + 3H_2O \text{ (photooxidation of } I^- \text{ and } IO_3^-) \quad (2)$$

$$2H^+ + 2e^- \rightarrow H_2 \text{ (photoreduction of } H^+ \text{ into } H_2) \quad (3)$$

$$IO_3^- + 6e^- + 3H_2O \rightarrow I^- + 6OH^- \text{ (photoreduction of } IO_3^- \text{ into } I^-) \quad (4)$$

$$4OH^- + 4h^+ \rightarrow O_2 + 2H_2O \text{ (photooxidation of } H_2O \text{ into } O_2) \quad (5)$$

In this system, the Fermi levels of Pt/ZrO_2/TaON and Pt/WO_3 do not match because of the lack of a physical connection between the two. Instead, they equilibrate reactive redox species in the reactant solution. More specifically, under the steady-state reaction conditions, the aligned Fermi level of Pt/ZrO_2/TaON equilibrates with respect to the redox potential of H^+/H_2. Similarly, the final alignment of the Fermi level of Pt/WO_3 is set at the redox potential of the IO_3^-/I^- pair. We also confirmed by ion chromatography that photooxidation of I^- ions into IO_3^- was occurring on unmodified ZrO_2/TaON, although a quantitative analysis was very difficult due to the small amount of product. This was consistent with the report by Nakamura et al., who claimed on the basis of photoelectrochemical analysis that valence band holes in TaON can efficiently oxidize I^- under band gap irradiation.[36] Taking into account these results and the fact that the loading of cocatalysts is required to achieve water splitting, it appears that the relatively inefficient process for this Z-scheme water splitting system is the water reduction process by ZrO_2/TaON rather than the oxidation of iodide ions and that water splitting results from the promotion of charge separation and H_2 formation in ZrO_2/TaON catalysts.

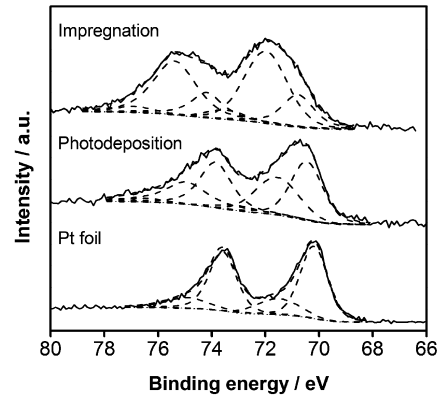

Figure 2. XPS spectra for Pt 4f of 1.0 wt % Pt-loaded ZrO_2/TaON prepared by photodeposition and impregnation methods. A spectrum of a Pt foil is shown for reference.

Because Pt was found to be the most effective cocatalyst among those examined (entry 6), the effect of Pt loading onto ZrO_2/TaON was investigated in more detail. When photodeposition was employed for Pt loading onto ZrO_2/TaON, the as-prepared sample did not function as efficiently as the impregnated sample did (entry 8). In particular, while stoichiometric H_2 and O_2 evolution was detected using the impregnated catalyst, the ratio of H_2 to O_2 evolution of the photodeposited catalyst was nonstoichiometric ($H_2/O_2 \approx 3$).

Changing the amount of Pt loaded onto the ZrO_2/TaON had a significant impact on the water splitting rate. With increasing Pt loading, the rates of H_2 and O_2 evolution both increased abruptly, reaching a maximum at 1.0 wt %, then decreasing (Table 1, entries 6, 9−12). In addition, the H_2/O_2 ratio of the products was close to 2 when the loading amount was more than 0.5 wt %. Thus, the method and amount of Pt cocatalyst loading were both important factors determining the efficiency of the two-step water-splitting system consisting of Pt/ZrO_2/TaON and Pt/WO_3 in the presence of IO_3^-/I^- shuttle redox mediator.

3.2. Electronic State and Morphology of the Loaded Platinum Species on ZrO_2/TaON. The strong effect of Pt loading on activity suggests differing physicochemical characteristics of the Pt-loaded samples. The electronic state of the loaded Pt species on ZrO_2/TaON was thus investigated by XPS. Figure 2 shows an XPS spectra for Pt 4f in 1.0 wt % Pt-loaded ZrO_2/TaON catalysts prepared by photodeposition and impregnation, along with reference data from a Pt foil. No appreciable difference in XPS peak positions was identified for the Zr 3d and Ta 4f spectra. The Pt 4f spectra could be resolved according to the previous study by Kim et al.[37] The spectrum for the Pt reference foil exhibited two major peaks with binding energies of ca. 70.2 and 73.6 eV, which were assigned to $4f_{7/2}$ and $4f_{5/2}$ electrons of metallic Pt (Pt^0), respectively. In addition to the Pt^0 state, two minor peaks, assignable to Pt with adsorbed oxygen ($Pt-O_{ads}$), were observed at binding energies of ca. 71.5

(36) Nakamura, R.; Tanaka, T.; Nakato, Y. *J. Phys. Chem. B* **2005**, *109*, 8920.

(37) Kim, K. S.; Winograd, N.; Davis, R. E. *J. Am. Chem. Soc.* **1971**, *93*, 6296.

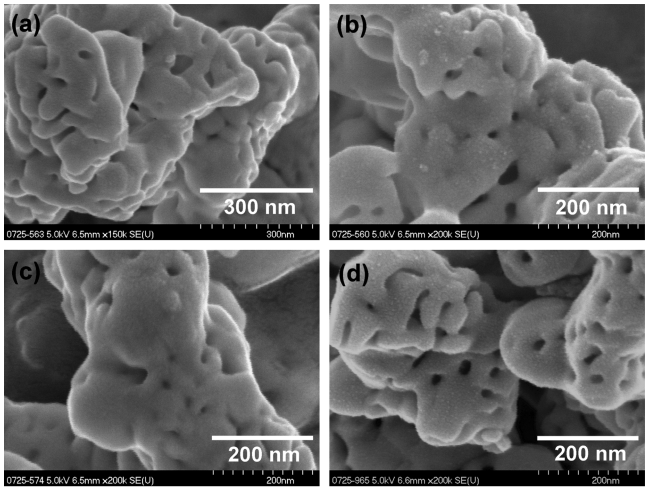

Figure 3. SEM image of 1.0 wt % Pt-loaded ZrO_2/TaON prepared by (b) photodeposition and (c) impregnation. Data for (a) unmodified ZrO_2/TaON is shown for reference. Image (d) indicates an analogue modified with 3.0 wt % Pt by impregnation.

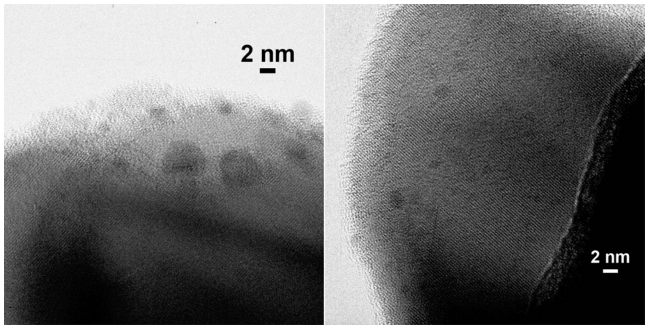

Figure 4. HR-TEM image of 1.0 wt % Pt-loaded ZrO_2/TaON prepared by impregnation.

and 74.9 eV. The Pt 4f spectra from the prepared catalysts also contained peaks assigned to Pt^0 and $Pt-O_{ads}$ species, with small contributions from $Pt^{II}O$ species appearing at binding energies of ca. 73.0−73.5 eV ($4f_{7/2}$ electrons). However, peaks assigned to Pt^0 and $Pt-O_{ads}$ species in the prepared catalysts were located at slightly higher binding energies than those of the Pt reference foil. This shift was more prominent in the impregnated sample than in the photodeposited sample. These results indicate that the loaded platinum species on ZrO_2/TaON were almost entirely metallic, but were somewhat electron-deficient.

SEM images of the same samples are shown in Figure 3. In the photodeposited catalyst, Pt was poorly dispersed on the ZrO_2/TaON surface, with some aggregation (Figure 3b). On the other hand, Pt nanoparticles smaller than 5 nm were highly dispersed in the impregnated catalyst, although they were somewhat difficult to observe (Figure 3c). When the loading amount of Pt was increased to 3.0 wt %, the surface coverage of Pt nanoparticles ~10 nm in size with ZrO_2/TaON became more distinct (Figure 3d). Therefore, the impregnation method allows for a higher dispersion of Pt nanoparticles on the surface of ZrO_2/TaON, compared to photodeposition.

Pt-loaded ZrO_2/TaON (1.0 wt %) was also investigated by HR-TEM. As shown in Figure 4, the Pt deposits dispersed on the ZrO_2/TaON were distinguishable due to the contrast in the images, which results from the difference in electron density between platinum and tantalum (or zirconium). As suggested by the corresponding SEM image (Figure 3c), the sample exhibited relatively good dispersion of Pt nanoparticles with a size of 2−5 nm, and ultrafine Pt dots smaller than 0.5 nm were also observable (Figure 4). It was also found that most of the loaded Pt nanoparticles are on the TaON component in the catalyst, as indicated by energy-dispersive X-ray spectroscopy analysis and the lattice-spacing of the base particle (Figure S2). However, some were also observed on the ZrO_2 component (see also the Supporting Information).

3.3. Relationship between the Structure and Activity of Pt-Loaded ZrO_2/TaON. As displayed in Table 1, the use of Pt-loaded ZrO_2/TaON catalysts prepared by impregnation (entry 6) resulted in a higher activity for Z-scheme water splitting, compared to an analogue derived from in situ photodeposition with the same Pt loading amount (entry 8). This difference in activity was primarily because of a more uniform dispersion and smaller Pt cocatalyst nanoparticles on the ZrO_2/TaON surface, as revealed by SEM and HR-TEM observations (Figures 3 and 4). It is a general trend in heterogeneous photocatalysis that highly dispersed catalytic species such as Pt lead to improved performance.[29,38,39] Another possible explanation for the difference in activity is the different electronic state of Pt loaded on ZrO_2/TaON. As shown in Figure 2, Pt nanoparticles in the impregnated catalyst were electron-deficient, in comparison to those on the photodeposited sample. Jin et al. and Cheng et al. reported the presence of electron-deficient Pt species in some Pt-impregnated TiO_2 catalysts, and the positive effects on photocatalytic activity were suggested.[40] Lee et al. also reported that such electron-deficient Pt on a semiconductor photocatalyst is advantageous as an electron collector.[41] Therefore, the difference in Pt valence should also contribute to the activity difference between the two catalysts. Specifically, the electron-deficient state of Pt in the impregnated catalyst may have led to the enhanced activity.

The amount of loaded Pt on ZrO_2/TaON has also a significant effect on the activity. On an increase of loading amount from 0 to 1.0 wt %, the water-splitting rate was markedly enhanced, and the ratio of H_2 to O_2 evolution became closer to stoichiometric ($H_2/O_2 \approx 2$). This enhancement in activity was due to the increase in the density of active sites for H_2 evolution, which is the relatively inefficient process for the Z-scheme overall water-splitting system using ZrO_2/TaON and WO_3 with an IO_3^-/I^- shuttle redox mediator. In the range between 1.0 and 3.0 wt % Pt loading, increasing the Pt amount had a negative effect on activity. It is likely that this decrease in activity with higher Pt loading was associated with excess coverage by Pt nanoparticles of the ZrO_2/TaON. The green color of the Pt-loaded samples became darker with increasing Pt loading, primarily due to excess coverage of the ZrO_2/TaON surface by Pt nanoparticles. As shown in Figures 3 and 4, the 1.0 wt % sample, which showed the highest activity (Table 1, entry 6), exhibited a relatively good dispersion of Pt nanoparticles smaller than 5 nm in size, while excess coverage by larger Pt nanoparticles was observed in the 3.0 wt % sample (Figure 3d). Such excess Pt loading can cause an inner-filter effect, thereby

(38) Maeda, K.; Teramura, K.; Saito, N.; Inoue, Y.; Domen, K. *J. Catal.* **2006**, *243*, 303.
(39) Zong, X.; Yan, H.; Wu, G.; Ma, G.; Wen, F.; Wang, L.; Li, C. *J. Am. Chem. Soc.* **2008**, *130*, 7176.
(40) (a) Li, Q.; Wang, K.; Zhang, S.; Zhang, M.; Yang, J.; Jin, Z. *J. Mol. Catal. A: Chem.* **2006**, *258*, 83. (b) Liu, G.; Yang, H. G.; Wang, X.; Cheng, L.; Lu, H.; Wang, L.; Lu, G. Q.; Cheng, H.-M. *J. Phys. Chem. C* **2009**, *113*, 21784.
(41) Jang, J. S.; Choi, S. H.; Kim, H. G.; Lee, J. S. *J. Phys. Chem. C* **2008**, *112*, 17200.

Table 2. Effect of O_2 Evolution Photocatalyst and Redox Mediator on the Rates of H_2 and O_2 Evolution in Z-Scheme Water Splitting using Pt (1.0 wt %)/ZrO_2/TaON as an H_2 Evolution Photocatalyst[a]

			activity[b]/μmol	
entry	catalyst	reactant soln	H_2	O_2
1	Pt/ZrO_2/TaON + Pt/WO_3	NaI	260	133
2	Pt/ZrO_2/TaON + Pt/WO_3	$FeCl_2$	0.9	0
3	Pt/ZrO_2/TaON + $BiVO_4$	$FeCl_2$	1.0	0
4	Pt/ZrO_2/TaON + $BiVO_4$	$FeCl_3$	0.7	42.4
5	Pt/ZrO_2/TaON + TiO_2 rutile	NaI	59.5	28.9
6[c]	Pt/ZrO_2/TaON + RuO_2/TaON	NaI	22.0	8.8
7	Pt/ZrO_2/TaON + $BiVO_4$	NaI	10.9	1.6
8	Pt/ZrO_2/TaON	NaI	7.4	0
9	Pt/ZrO_2/TaON	$FeCl_2$	0.4	0

[a] Reaction conditions: catalyst, 50 mg of Pt/ZrO_2/TaON or 100 mg of an O_2 evolution photocatalyst; aqueous solution, 100 mL (1.0 mM); light source, xenon lamp (300 W) fitted with a cold mirror (CM-1); reaction vessel, Pyrex top-irradiation type; irradiation wavelength, $350 < \lambda < 800$ nm. [b] Total amount of gas evolution after 5 h. [c] RuO_2/TaON 50 mg, NaI 0.2 mM.

contributing to a decrease in activity.[5e,42−44] It is also noted that both H_2 oxidation and O_2 reduction occur efficiently on a Pt electrode, as demonstrated by our recent electrochemical measurements.[45] Considering that the primary role of Pt in the present Z-scheme water splitting system is to act as electron collector and to offer active sites for the reduction of H^+ and IO_3^- on each photocatalyst, the contribution of O_2 reduction would be larger than that of H_2 oxidation. Nevertheless, there is the possibility that photogenerated holes can migrate to the loaded Pt on a photocatalyst.[46] In any cases, the negative effect of these undesirable reactions on Z-scheme activity is expected to be more pronounced at higher Pt loading conditions.

One may feel that the present optimal loading of Pt, 1.0 wt %, is too large for ZrO_2/TaON, having relatively low specific surface area (ca. 5 $m^2\ g^{-1}$). Previous studies revealed that the optimal loading amount of a given cocatalyst is dependent on various factors, including the type of base photocatalyst, the loaded cocatalyst, and photocatalytic reaction.[13b,14b,38,43,47,48] It is also suggested by our recent kinetic assessment on water splitting using $(Ga_{1-x}Zn_x)(N_{1-x}O_x)$ that the amount of the optimal loading for a given photocatalyst may be dependent on the number of accumulated photons in photocatalyst particles.[13e]

3.4. Effect of O_2 Evolution Photocatalyst and Redox Mediator. Table 2 lists the activities of two-step water splitting systems under UV and visible irradiation ($350 < \lambda < 800$ nm) in which 1.0 wt % Pt-loaded ZrO_2/TaON was used as a building block for H_2 evolution with various O_2 evolution photocatalysts (Pt/WO_3, TiO_2 rutile, RuO_2/TaON, or $BiVO_4$). It has been reported that the Fe^{3+}/Fe^{2+} redox couple acts as an effective electron mediator for some two-step water-splitting systems consisting of Rh-doped $SrTiO_3$ (H_2 evolution system) and an O_2 evolution photocatalyst such as $BiVO_4$ or WO_3.[16,20,25,29] Interestingly, however, the combination of Pt/ZrO_2/TaON with either Pt/WO_3 or $BiVO_4$ produced no appreciable H_2 and O_2 from an aqueous solution containing Fe^{2+} as an electron donor (entries 2 and 3). Although the use of $FeCl_3$ as a starting redox mediator for the Pt/ZrO_2/TaON + $BiVO_4$ system instead of $FeCl_2$ resulted in appreciable O_2 evolution (entry 4), H_2 was produced simultaneously on the same order as in the case of Fe^{2+} (entry 3). These results suggest that photooxidation of Fe^{2+} does not proceed efficiently on Pt/ZrO_2/TaON. When Pt/ZrO_2/TaON and NaI were respectively employed as an H_2 evolution photocatalyst and an electron mediator, on the other hand, all of the tested O_2 evolution photocatalysts achieved water splitting (entries 5−7).

It appeared that these characteristic behaviors in reactivity with respect to O_2 evolution photocatalysts and redox mediators arise primarily from the different reactivities of Pt/ZrO_2/TaON with the redox mediators employed. To examine this possibility, H_2 evolution by Pt/ZrO_2/TaON alone in the presence of NaI or $FeCl_2$ as an electron donor was investigated. As given in Table 2, Pt/ZrO_2/TaON produced appreciable H_2 from aqueous NaI solution (entry 8), while the amount of H_2 evolved from aqueous $FeCl_2$ solution was negligible (entry 9). These results indicate that I^- ions undergo oxidation by reacting with holes in the valence band of Pt/ZrO_2/TaON, while Fe^{2+} ions do not. The successful conversion of I^- into IO_3^- by Pt/ZrO_2/TaON allowed for simultaneous H_2 and O_2 evolution in combination with the tested O_2 evolution photocatalysts, because they were all active for the reduction of IO_3^- into I^- under band-gap irradiation.[15,28] Inefficient O_2 evolution was observed from RuO_2/TaON and $BiVO_4$ because water oxidation by these materials is significantly suppressed in the presence of I^-, even at the low levels resulting from the preferential oxidation of I^-.[15,28] Therefore, Pt/ZrO_2/TaON is a useful component for H_2 evolution in two-step water splitting with an IO_3^-/I^- redox mediator.

3.5. Effect of Reaction Conditions. Photocatalytic reaction conditions such as redox concentration and pH are known to have significant effects on water-splitting activity.[15,25,48] In one-step photoexcitation systems, for example, (oxy)nitrides exhibit a unique pH dependence, very different from the general character of transition metal oxide based photocatalysts.[2d,3c,48] However, no such information on two-step water splitting using an (oxy)nitride photocatalyst component was available. Therefore, the effect of reaction conditions was investigated for the most active combination of Pt/ZrO_2/TaON and Pt/WO_3. Figure 5 shows the time courses of H_2 and O_2 evolution for a mixture of 1.0 wt % Pt-loaded ZrO_2/TaON and Pt/WO_3 under visible light ($420 < \lambda < 800$ nm). The reactions were conducted for 10 h with an intermediate evacuation after 5 h of irradiation. The average rates of H_2 and O_2 evolution achieved in the second 5 h run are summarized in Table 3. No gas evolution was observed in the absence of NaI. With increasing NaI concentration, the rates of H_2 and O_2 evolution both improved significantly, reaching a maximum at 1.0 mM and then decreasing gradually. Although the rates of H_2 and O_2 evolution did not satisfy the exact stoichiometry at the beginning of the reaction under all conditions examined, the H_2/O_2 ratio tended toward stoichiometric with longer reaction times. This may be due to the accumulation of IO_3^- in the solution up to a certain level.[28] The highest performance was obtained using 1.0 mM NaI. As mentioned earlier, the relatively inefficient step for this reaction system was the water reduction process on Pt-loaded ZrO_2/TaON catalysts. Therefore, the appreciable enhancement of gas

(42) Reber, J. F.; Meier, K. *J. Phys. Chem.* **1986**, *90*, 824.
(43) Ohtani, B.; Iwai, K.; Nishimoto, S.; Sato, S. *J. Phys. Chem. B* **1997**, *101*, 3349.
(44) Bao, N.; Shen, L.; Takata, T.; Domen, K. *Chem. Mater.* **2008**, *20*, 110.
(45) Yoshida, M.; Takanabe, K.; Maeda, K.; Ishikawa, A.; Kubota, J.; Sakata, Y.; Ikezawa, Y.; Domen, K. *J. Phys. Chem. C* **2009**, *113*, 10151.
(46) Yoshida, M.; Yamakata, A.; Takanabe, K.; Kubota, J.; Osawa, M.; Domen, K. *J. Am. Chem. Soc.* **2009**, *131*, 13218.
(47) Sayama, K.; Arakawa, H. *J. Chem. Soc., Faraday Trans.* **1997**, *93*, 1647.
(48) (a) Maeda, K.; Teramura, K.; Masuda, H.; Takata, T.; Saito, N.; Inoue, Y.; Domen, K. *J. Phys. Chem. B* **2006**, *110*, 13107. (b) Maeda, K.; Saito, N.; Lu, D.; Inoue, Y.; Domen, K. *J. Phys. Chem. C* **2007**, *111*, 4749.

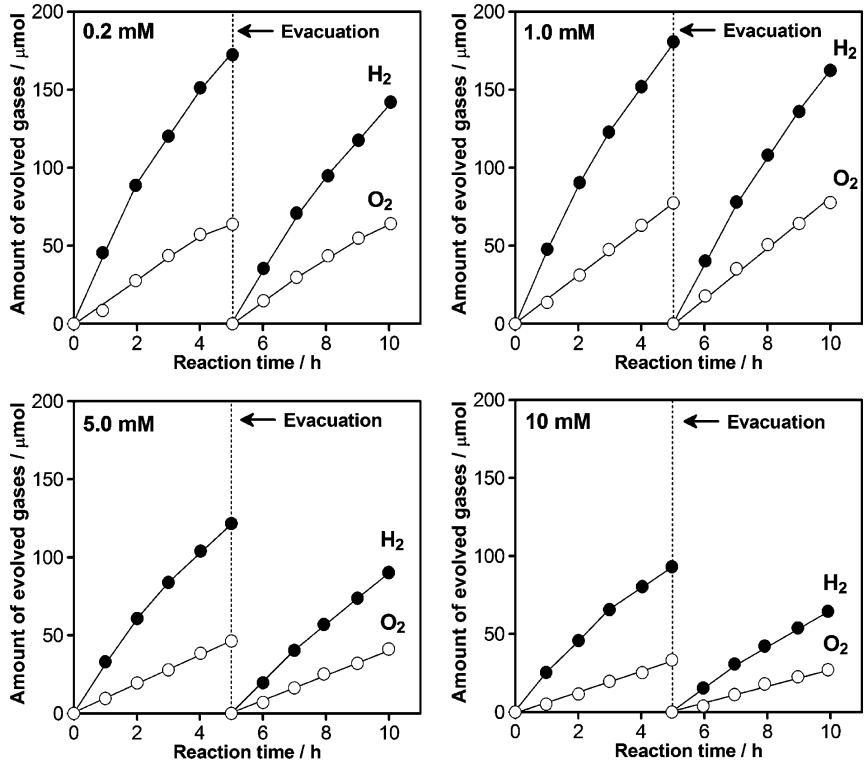

Figure 5. Dependence of the rates of H_2 and O_2 evolution over a mixture of Pt/WO_3 and $Pt/ZrO_2/TaON$ on the concentration of NaI in the reactant solution. Reaction conditions: catalyst, 100 mg of Pt/WO_3 and 50 mg of $Pt/ZrO_2/TaON$; aqueous NaI solution, 100 mL; light source, xenon lamp (300 W) fitted with a cold mirror (CM-1) and a cutoff filter (L42); reaction vessel, Pyrex top-irradiation type; irradiation wavelength, $420 < \lambda < 800$ nm. Pt (1.0 wt %) was deposited on $ZrO_2/TaON$ by impregnation.

Table 3. Effect of NaI Concentration and Reaction pH on the Rates of H_2 and O_2 Evolution over a Mixture of Pt (1.0 wt %)/ZrO_2/TaON and Pt/WO_3 with IO_3^-/I^- Shuttle Redox Mediator[a]

			gas evolution rate[b]/μmol h^{-1}		
entry	concn of NaI/mM	pH	H_2	O_2	H_2/O_2 ratio
1	0	no control[c]	0	0	
2	0.2	no control[c]	28.3	12.8	2.21
3	1.0	no control[c]	32.6	15.6	2.09
4	5.0	no control[c]	18.1	8.4	2.19
5	10	no control[c]	13.0	5.5	2.37
6	1.0	3.0[d]	14.3	6.0	2.40

[a] Reaction conditions: catalyst, 50 mg of $Pt/ZrO_2/TaON$ and 100 mg of Pt/WO_3; aqueous NaI solution, 100 mL; light source, xenon lamp (300 W) fitted with a cold mirror (CM-1) and a cutoff filter (L42); reaction vessel, Pyrex top-irradiation type; irradiation wavelength, $420 < \lambda < 800$ nm. [b] Average rates of gas evolution in 5 h for the second run (see Figure 5). [c] Approximately pH 5.4. [d] Adjusted by H_2SO_4.

evolution rates was due to the promotion of H_2 evolution on Pt-loaded $ZrO_2/TaON$ catalysts by the addition of NaI. However, excess NaI addition had a negative effect on activity, along with a pronounced deviation in the H_2/O_2 ratio. A previous study demonstrated that the competitive oxidation of I^- (backward reaction of eq 4) with water oxidation (eq 5) occurs on Pt/WO_3 when the concentration of I^- becomes high, thereby decreasing the rate of O_2 evolution.[15] As a result, the water-splitting rate gradually decreased with increasing NaI concentration above 1.0 mM. Note that the degree of the activity increase observed at lower NaI concentration range (~0.2−1.0 mM) in the present case is significant, in comparison to a similar IO_3^-/I^--based Z-scheme system consisting of Pt-loaded $SrTiO_3$ codoped with Cr/Ta (H_2 evolution system) and Pt/WO_3 (O_2 evolution system) under visible light.[15] In that system, the optimal NaI concentration is 5−10 mM, which is much higher than that in the present system (1.0 mM). This is probably because of the efficient ability of $Pt/ZrO_2/TaON$ to oxidize iodide ions, as suggested by the fact that the addition of a small amount of NaI (0.2 mM) results in an abrupt activity increase. This idea is also consistent with the results of photoelectrochemical measurements.[36]

It has also been reported that the pH of the reactant solution affects the overall efficiency of Z-scheme water splitting in the presence of an IO_3^-/I^- shuttle redox mediator, as does the concentration of NaI.[15] When Pt/WO_3 is applied as an O_2 evolution photocatalyst in the Z-scheme system, basic conditions (pH >7) are undesirable, because WO_3 is inherently unstable in basic media.[15,20b] We thus attempted to examine the effect of the reaction pH on activity in the present system for a pH of 7 and below. However, it was difficult to adjust the reaction pH to values above 5.4 (achieved without control) because of a buffering effect of the mixture of $Pt/ZrO_2/TaON$ and Pt/WO_3. Therefore, the pH effect was investigated below pH 5.4. As given in Table 3 (entry 6), lowering the pH from 5.4 to 3.0 by H_2SO_4 resulted in a decrease in water-splitting rate and an increased H_2/O_2 production ratio. It is generally known that products generated as a result of photooxidation of I^- ions are strongly dependent on the reaction pH. In addition to reaction 2, there is another reaction path for the oxidation of I^- by valence band holes in a photocatalyst, as follows:[15]

$$3I^- + 2h^+ \rightarrow I_3^- \text{ (photooxidation of } I^- \text{ into } I_3^-) \qquad (6)$$

I_3^- produced by eq 6 does not act as an effective electron acceptor for O_2 evolution by Pt/WO_3.[15] Therefore, a higher pH is preferable for reaction 2 to proceed. It should be stressed that a red-brown solid was deposited on the wall of the closed-

gas circulation system after reaction at pH 3.0, suggesting that iodine (I_2) was generated from I_3^- according to the equilibrium

$$I_3^- \leftrightarrow I^- + I_2 \quad (7)$$

The reaction was carried out under reduced pressure, which promoted the sublimation of I_2 from the liquid suspension, but no significant deposition of I_2 was observed at pH 5.4. It is therefore likely that eq 6 occurs on the surface of ZrO_2/TaON at lower pH conditions, in competition with eq 2, which produces IO_3^- as an effective electron acceptor for Pt/WO_3. I_3^- ions are also converted into I^- and IO_3^- via the disproportionation reaction[49]

$$3I_3^- + 3H_2O \rightarrow 8I^- + IO_3^- + 6H^+ \quad (8)$$

This reaction proceeds more smoothly under basic reaction conditions than under acidic conditions. As a result, the H_2/O_2 ratio in the reaction products would become larger than stoichiometric, even at the optimal NaI concentration.

In all reactions conducted, the rates of H_2 and O_2 evolution decreased slightly with time but recovered after the initial stage of the second run, suggesting that H_2-O_2 recombination, which is thermodynamically favorable, takes place during the reaction. This was confirmed by testing the water formation reaction from a mixture of H_2 and O_2 in the dark using Pt/ZrO_2/TaON and Pt/WO_3 catalysts. As shown in Figure S3, the amounts of H_2 and O_2 in a closed-gas circulation system both decreased with time while the stoichiometric ratio was maintained, indicating that water formation (eq 9) occurs on a mixture of Pt/ZrO_2/TaON and Pt/WO_3.

$$2H_2 + O_2 \rightarrow 2H_2O \quad (9)$$

It is thus clear that, during photocatalytic water splitting, this undesirable reaction occurs, thereby reducing the detected rates of H_2 and O_2 evolution.

On the basis of these results, careful refinement of the cocatalyst-loading and reaction conditions is very important for efficient water splitting using ZrO_2/TaON as a building block for H_2 evolution in a Z-scheme system with Pt/WO_3 (O_2 evolution photocatalyst) and an IO_3^-/I^- shuttle redox mediator. It is also important to examine the photoresponse of a given photocatalytic reaction with respect to the incident light wavelength. Figure 6 shows the dependence of the rates of H_2 and O_2 evolution on the wavelength of the incident light. The H_2 and O_2 evolution rates both decreased as the cutoff wavelength increased. The longest wavelengths available for H_2 and O_2 evolution were 500 and 440 nm, respectively, which are consistent with the absorption edges of ZrO_2/TaON and WO_3. The total amount of evolved H_2 and O_2 from 1.0 mM NaI solution under >420 nm irradiation (ca. 500 μmol, see Figure 5) was much larger than the amount of NaI present (100 μmol). Taken together, it is clear that the water splitting reaction proceeds photocatalytically via light absorption by these two materials according to the Z-scheme principle.

3.6. AQY Measurements. The AQY for photocatalytic reactions is a more reliable measure of activity than the rate of gas evolution under the given reaction conditions. First, we measured the AQY for overall water splitting under the same conditions as for Figure 5, but with monochromatic light (420.5 nm), obtaining an AQY of 2.8 ± 0.2%.[50] As mentioned earlier, undesirable water formation from H_2 and O_2 occurs in the present reaction system, so that only the H_2 and O_2 molecules that avoid water formation in the suspension are able to contribute to the AQY. This implies that the AQY would be improved by reducing the concentration of photocatalysts in the suspension, due to a decrease in the opportunity for undesirable backward reactions. Also, the number of gas molecules produced by the reaction would inevitably become small when the number of incident photons is small. This situation was expected to increase the negative effect of water formation in the liquid phase, in comparison to the same system under stronger irradiation.

Therefore, reactions for AQY measurement were performed using a Pt/ZrO_2/TaON−Pt/WO_3−NaI mixture while maintaining a weight ratio of 50−100−15 (mg).[51] As given in Table 4, the AQY was improved as the weight ratio decreased from 25 to 50−7.5 (entry 2), below which it dropped slightly (entry 3).

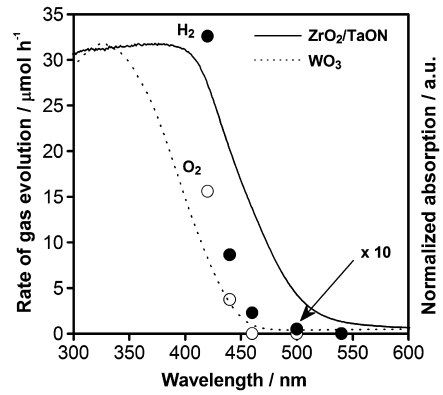

Figure 6. Dependence of the rates of H_2 and O_2 evolution over a mixture of Pt/WO_3 and Pt/ZrO_2/TaON on the incident light wavelength. Reaction conditions: catalyst, 100 mg of Pt/WO_3 and 50 mg of Pt/ZrO_2/TaON; aqueous NaI solution, 100 mL (1.0 mM); light source, xenon lamp (300 W) fitted with a cold mirror (CM-1) and a given cutoff filter; reaction vessel, Pyrex top-irradiation type. Pt (1.0 wt %) was deposited on ZrO_2/TaON by impregnation.

Table 4. Effect of the Weight Ratio of Pt/ZrO_2/TaON−Pt/WO_3−NaI in the Reactant Solution on Water-Splitting Activity under Monochromatic Light Irradiation (λ = 420.5 nm)[a]

entry	Pt/ZrO_2/TaON−Pt/WO_3−NaI/mg	concn of NaI/mM	loading amt of Pt on ZrO_2/TaON/wt %	gas evolution rate[b]/μmol h^{-1}		
				H_2	O_2	AQY[c]/ %
1	50−100−15	1.0	1.0	3.3	1.6	2.7
2	25−50−7.5	0.5	1.0	5.5	2.7	4.3
3	10−20−3.0	0.2	1.0	4.6	2.1	3.5
4	10−20−15	1.0	1.0	4.3	1.4	2.3
5	25−50−7.5	0.5	0.5	7.5	3.8	6.3
6	25−50−7.5	0.5	0.1	<1	n.d.	

[a] Reaction conditions: catalyst, Pt/ZrO_2/TaON and Pt/WO_3; aqueous NaI solution, 100 mL; light source, xenon lamp (300 W) fitted with a cold mirror (CM-1) and a band-pass filter; reaction vessel, Pyrex top-irradiation type. [b] Steady rates of gas evolution with an experimental error of ~10%. [c] Calculated according to eq 1 on the basis of O_2 evolution rate.

(49) Dushman, P. *J. Phys. Chem.* **1904**, *8*, 481.

(50) The corresponding time course is shown in Figure S4 (see the Supporting Information). Reproducibility tests using different batches of Pt/ZrO_2/TaON showed that the obtained AQY slightly varied from batch to batch but remained within 10%. Because the ratio of H_2 to O_2 evolution was sometimes slightly higher than that expected from the stoichiometry, we calculated the AQYs on the basis of the rates of O_2 evolution derived from the two-step water splitting cycle.

(51) In this case, the NaI concentration was 1.0 mM (15 mg in 100 mL of solution).

When the weight ratio of photocatalysts was reduced without changing the NaI concentration, however, the AQY did not improve (entry 4). This is because photooxidation of I^- occurs on Pt/WO_3, thereby suppressing water oxidation, as mentioned earlier. We also reduced the concentration of Pt nanoparticles loaded on ZrO_2/TaON from 1.0 wt % to 0.5 wt % while maintaining the optimal weight ratio, and an AQY of 6.3% was obtained (entry 5). However, the AQY became immeasurably low below this level of Pt loading, because the rates of H_2 and O_2 evolution were very low (entry 6).

The AQY of the present reaction system was strongly dependent on the component concentrations. The increase in AQY with decreasing weight ratio was attributed to the decreased probability of H_2-O_2 recombination on each photocatalyst. On the other hand, further reduction of the weight ratio contributed to a decrease in AQY, presumably because the photocatalytic suspension did not fully absorb the photon flux from the light source. According to these results, H_2-O_2 recombination in the liquid phase is significant. Therefore, it is very important to design the reaction system carefully in order to utilize a weak light source, such as sunlight.

3.7. Reason for the High Activity. The AQY value obtained through the above refinement was the highest value for a visible-light-driven overall water splitting system reported to date. For Z-scheme water-splitting systems in particular, the AQY of our system was greater than that of the previous reported system consisting of Rh-doped $SrTiO_3$ and $BiVO_4$ (4.3% at 420 nm).[52] This implied that a similar enhancement of AQY in other systems might be achieved with an appropriate refinement of the reaction conditions. We therefore conducted a similar refinement of TaON prepared in a manner similar to that for ZrO_2/TaON. Even with the optimal weight ratio of each component, Pt/TaON had an activity 6 times lower than that of Pt/ZrO_2/TaON (Figure S5).[53] This clearly demonstrated that the high activity of the ZrO_2/TaON-based system was not a direct result of the system refinement but was due to some other factors.

The primary requirement to achieve a high efficiency in a Z-scheme water-splitting system is to suppress undesirable but thermodynamically favorable backward reactions involving redox couples.[15,25] In an IO_3^-/I^- redox system, for example, IO_3^- and I^- ions are respectively more susceptible to reduction and oxidation on H_2- and O_2-evolution photocatalysts than on protons and water molecules. The rate of H_2 evolution on Pt/ZrO_2/TaON from aqueous NaI solution decreased gradually with reaction time, and the addition of $NaIO_3$ into the suspension resulted in a significant drop in the H_2 evolution rate (Figure S6). This is clear evidence that reduction of IO_3^- ions on Pt/ZrO_2/TaON occurs more efficiently than water reduction. When Pt/WO_3 powder is cosuspended in an aqueous NaI solution containing Pt/ZrO_2/TaON powder, however, the excellent performance of Pt/WO_3 for the reduction of IO_3^- ions, as indicated by a previous study,[15] should help Pt/ZrO_2/TaON reduce water to produce H_2. This idea is supported by the observation that the rate of H_2 evolution from a mixture of Pt/ZrO_2/TaON and Pt/WO_3 (Table 2, entry 1) was much higher than from Pt/ZrO_2/TaON alone (Table 2, entry 8). The efficient reduction behavior of Pt/ZrO_2/TaON for IO_3^- ions also suggests that Pt/ZrO_2/TaON would evolve O_2 from aqueous solution containing IO_3^- ions. However, no such O_2 evolution was detected. This indicates that photooxidation of I^- ions occurs preferentially on Pt/ZrO_2/TaON, thereby suppressing the photooxidation of water to produce O_2. In other words, Pt/ZrO_2/TaON has strong tendency to oxidize I^- ions.[36] Although Pt/WO_3 exhibited excellent activity for O_2 evolution from aqueous $NaIO_3$ solution, the addition of I^- ions into an aqueous $NaIO_3$ solution containing Pt/WO_3 powder resulted in a drop in the O_2 evolution rate. This was because the photooxidation of I^- ions on Pt/WO_3 competes with that of water.[15] This can be overcome in the presence of Pt/ZrO_2/TaON, a good I^- scavenger. To summarize, both H_2 and O_2 evolution photocatalysts, Pt/ZrO_2/TaON and Pt/WO_3, help each other to enable the forward reactions to proceed efficiently, minimizing undesirable backward reactions involving the IO_3^-/I^- redox couple on each photocatalyst. As a result, visible-light water splitting over the mixture can proceed with higher quantum yield.

However, Pt/TaON is also an efficient scavenger of I^- ions, as indicated by previous studies.[26,28,36] Therefore, the high activity of the present Pt/ZrO_2/TaON and Pt/WO_3 system cannot be explained completely in terms of the reactivity with I^- ions. As shown in Figure 1, UV−visible spectroscopy indicated a slight blue shift of the absorption edge of TaON by the formation of a composite with ZrO_2. This was also confirmed by plotting $(\alpha h\nu)^{1/2}$ with respect to $h\nu$, where α, h, and ν are absorption coefficient (equivalent to Kubelka−Munk function), Planck constant, and light frequency (Figure S7). According to the previous report,[54] we assumed that both TaON and ZrO_2/TaON are indirect band gap semiconductors. However, XRD analysis showed that the positions of diffraction peaks of ZrO_2/TaON remained unchanged, in comparison to TaON alone (Figure S8). It indicated that interfacial diffusion of ZrO_2 into the TaON matrix (even if it occurred) was not large enough to form the solid solution phase of ZrO_2 and TaON, even though the crystal structures of the two are very similar (monoclinic baddelyite-type structure).[55] Nevertheless, it is likely that the blue shift of absorption edge in ZrO_2/TaON is attributable to slight interfacial diffusion of ZrO_2 into the TaON lattice. The bottom of the conduction band (−1.0 V, vs NHE at pH 0) of ZrO_2 is more negative than that of TaON (−0.3 V).[35,56] Therefore, the potential of the conduction band bottom of TaON should lift up to more negative potential when ZrO_2 is introduced into TaON to form a solid solution phase. The enlarged band gap of ZrO_2-TaON solid solutions has been reported by previous studies.[55a,b] The slightly more negative potential of the conduction band of ZrO_2/TaON might contribute to the enhanced activity, because of the stronger thermodynamic driving force toward the reduction of water.

Another possible explanation for the high activity resulting from ZrO_2/TaON is that the material has a lower defect density, as indicated by the weaker background level in the UV−visible spectrum than is the case for TaON (Figure 1). The increased background level in the TaON spectrum is due to reduced

(52) Kudo, A. "Nano-structured Photocatalysts for Solar Water Splitting", ICACC Symposium 74th International Symposium on Nanostructured Materials and Nanocomposites: Development and Applications, Dayton Beach, FL, USA, January 28, 2010.

(53) As shown in Figure S5, no O_2 evolution was observed in the initial stage of the reaction, due primarily to the detection limit of our gas chromatograph. The AQYs calculated from the initial H_2 evolution rate and the O_2 evolution rate were ca. 1 and 0.2%, respectively.

(54) Fang, C. M.; Orhan, E.; Wijs, G. A.; Hintzen, H. T.; Groot, R. A.; Marchand, R.; Saillard, J.-Y.; With, G. *J. Mater. Chem.* **2001**, *11*, 1248.

(55) (a) Grins, J.; Käll, P.; Svensson, G. *J. Mater. Chem.* **1994**, *4*, 1293. (b) Guenther, E.; Jansen, M. *Mater. Res. Bull.* **2001**, *36*, 1399. (c) Yashima, M.; Lee, Y.; Domen, K. *Chem. Mater.* **2007**, *19*, 588.

(56) Chun, W. A.; Ishikawa, A.; Fujisawa, H.; Takata, T.; Kondo, J. N.; Hara, M.; Kawai, M.; Matsumoto, Y.; Domen, K. *J. Phys. Chem. B* **2003**, *107*, 1798.

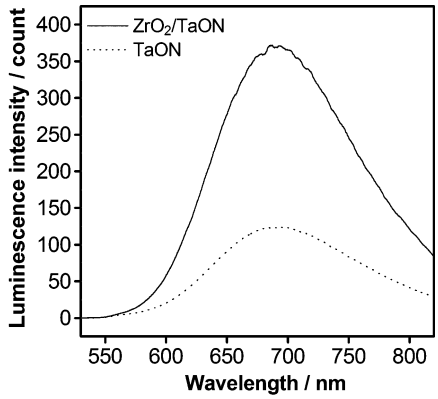

Figure 7. Photoluminescence spectra measured at liquid-nitrogen temperature for TaON and ZrO_2−TaON. The excitation wavelength was 420 nm.

tantalum species (e.g., Ta^{4+} and Ta^{3+}), which can act as traps for photogenerated electrons and holes,[57] although XPS analysis did not detect such lower valence tantalum species, presumably due to the detection limit. The difference in UV−visible spectra indicates that ZrO_2/TaON has a lower density of surface defects and hence exhibits higher photocatalytic performance than TaON. The relationship between photocatalytic activity and the background level in the UV−visible spectra has also been qualitatively documented in Ta_3N_5[57] and Ge_3N_4.[58] Specifically, the activity tends to increase with a decrease in the background level of the UV−visible spectra.

The contribution of such surface defects to the fate of photogenerated charge carriers in TaON and ZrO_2/TaON was examined by photoluminescence spectroscopy. As shown in Figure 7, the result showed that both TaON and ZrO_2/TaON exhibit a luminescence band centered at ca. 690 nm upon photoexcitation of 420 nm photons. However, the luminescence intensity of ZrO_2/TaON is ca. 3 times larger than that of TaON, even though the penetration of the incident photons are partially blocked by the ZrO_2 component that cannot be excited by 420 nm photons. This result might be explained in terms of the reduced density of nonradiative recombination sites in ZrO_2/TaON; more specifically, donor levels, formed by the reduced Ta species, below the conduction band of TaON would act as effective traps of photogenerated carriers. The identical trend in photoluminescence and photocatalytic activity has been reported in Ge_3N_4 photocatalyst.[58a]

To further investigate the properties of ZrO_2/TaON, photoelectrochemical measurements were carried out using a porous ZrO_2/TaON electrode.[59,60] Interestingly, the ZrO_2/TaON electrode generated both cathodic and anodic photocurrents under intermittent visible light, as shown in Figure 8, which were assignable to water reduction and oxidation, respectively. A TaON electrode prepared in the same manner exhibited only an anodic photocurrent based on water oxidation (Figure 8) and showed n-type semiconducting character, consistent with previous studies.[36,61] Although the photoelectrochemical properties of (oxy)nitrides for water splitting have been extensively investigated during the development of water-splitting photocatalysts,[36,57,61,62] no behavior similar to that of ZrO_2/TaON has yet been reported.

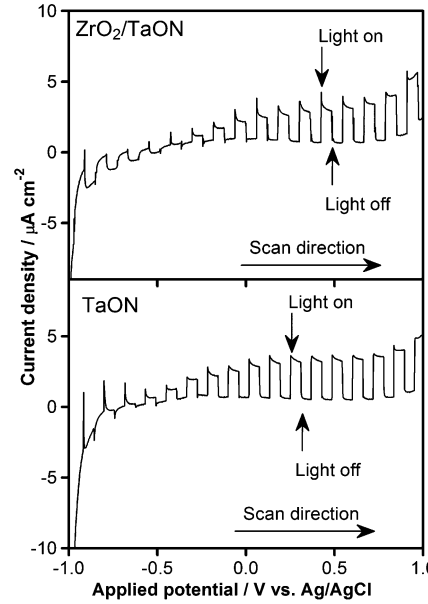

Figure 8. Current−voltage curves for porous ZrO_2/TaON and TaON electrodes under intermittent visible irradiation ($420 < \lambda < 800$ nm) in 0.1 M Na_2SO_4 solution. Scan rate: 20 mV s^{-1}.

TaON powder was prepared by heating Ta_2O_5 at 1123 K for 15 h under a flow of NH_3. During this process, the production of many nitrogen vacancies is expected, because the conversion of metal oxide into oxynitride and the concomitant decomposition of the oxynitride occur simultaneously at such high temperatures.[63] Along with the production of nitrogen vacancies, some reduced tantalum species are generated in order to maintain charge neutrality in the material. This is in good agreement with UV−visible spectroscopy measurements, which showed that the present TaON had an increased background level in the spectrum (Figure 1). The defects related to the

(57) Maeda, K.; Nishimura, N.; Domen, K. *Appl. Catal. A: Gen.* **2009**, *370*, 88.

(58) (a) Lee, Y.; Watanabe, T.; Takata, T.; Hara, M.; Yoshimura, M.; Domen, K. *J. Phys. Chem. B* **2006**, *110*, 17563. (b) Maeda, K.; Saito, N.; Inoue, Y.; Domen, K. *Chem. Mater.* **2007**, *19*, 4092.

(59) Porous ZrO_2/TaON and TaON electrodes were prepared by pasting viscous slurry onto conducting glass according to a previously described method.[61] A mixture of 50 mg of as-prepared ZrO_2/TaON (or TaON) powder (particle size 300−500 nm), 10 μL of acetylacetone (Kanto Chemicals), 10 μL of TritonX (Aldrich), 10 μL of poly(ethylene glycol) 300 (Kanto Chemicals), and 250 μL of distilled water was ground in an agate mortar to prepare the viscous slurry. The slurry was then pasted onto fluorine-doped tin oxide (FTO) glass slides (12 Ω sq^{-1}, transparency 80%, thickness 1 mm; Asahi Glass, Japan) to prepare a 1×4 cm^2 electrode, and the sample was calcined in a nitrogen gas flow at 673 K for 1 h. Thermogravimetric and differential thermal analysis revealed that almost no carbon species, derived from additives in the preparation, are persistent in the as-prepared electrode.

(60) Measurements were performed using a conventional Pyrex electrochemical cell with a platinum wire as a counter electrode and an Ag/AgCl reference electrode under potentiostat control (HSV-100, Hokuto Denko, Japan). Current−voltage curves were measured in an aqueous sodium sulfate solution (Na_2SO_4, 0.1 M, 100 mL) as a supporting electrolyte. The electrolyte solution was purged with nitrogen prior to the measurements and was maintained at room temperature by a flow of cooling water during the measurements. A 300 W xenon lamp fitted with a cutoff filter was used as a visible light irradiation source. The effective irradiation area was 1×3.5 cm^2.

(61) Abe, R.; Takata, T.; Sugihara, H.; Domen, K. *Chem. Lett.* **2005**, *34*, 1162.

(62) (a) Ishikawa, A.; Takata, T.; Kondo, J. N.; Hara, M.; Domen, K. *J. Phys. Chem. B* **2004**, *108*, 11049. (b) Maeda, K.; Hashiguchi, H.; Masuda, H.; Abe, R.; Domen, K. *J. Phys. Chem. C* **2008**, *112*, 3447. (c) Le Paven-Thivet, C.; Ishikawa, A.; Ziani, A.; Le Gendre, L.; Yoshida, M.; Kubota, J.; Tessier, F.; Domen, K. *J. Phys. Chem. C* **2009**, *113*, 6157. (d) Hashiguchi, H.; Maeda, K.; Abe, R.; Ishikawa, A.; Kubota, J.; Domen, K. *Bull. Chem. Soc. Jpn.* **2009**, *82*, 401.

(63) Orhan, E.; Tessier, F.; Marchand, R. *Solid State Sci.* **2002**, *4*, 1071.

reduced Ta species and/or anionic vacancies form a donor level slightly below the bottom of the conduction band, which is the origin of the n-type semiconducting character of TaON.[36,61] Accordingly, the observed photoresponse in the ZrO_2/TaON electrode, which produced both cathodic and anodic photocurrents, clearly indicates that the n-type semiconducting character of TaON is moderated by the formation of a composite with ZrO_2. In other words, the generation of defects related to the reduced Ta species and/or nitrogen vacancies at the TaON surface is suppressed by prior modification of Ta_2O_5 with ZrO_2. This is in good agreement with the lower background level in the UV−visible spectrum of ZrO_2/TaON than in the TaON spectrum (Figure 1).

There are two possible explanations for the origin of the cathodic photocurrent, indicating a p-type semiconducting character, observed in the ZrO_2/TaON electrode. The first is that the present ZrO_2/TaON is nearly an intrinsic semiconductor, resulting in the generation of both cathodic and anodic photocurrents upon polarization of the electrode. The second is that ZrO_2/TaON possesses two different compositional regions in the material, which give rise to p- and n-type semiconducting characters, respectively. ZrO_2/TaON composite was prepared by heating ZrO_2/Ta_2O_5 at 1123 K for 15 h under a flow of NH_3 through the transformation of Ta_2O_5 into TaON, while the ZrO_2 component did not undergo nitridation.[31,64] The p-type photoresponse might result from TaON component doped with Zr^{4+} ions, which are diffused from the ZrO_2 modifier. Although our structural analysis by XRD, XPS, HR-TEM, and X-ray absorption spectroscopy could not detect interfacial diffusion of Zr^{4+} ions into TaON,[31] the structural similarity of TaON with respect to ZrO_2 could allow for interfacial diffusion at the atomic scale during nitridation.[55] This idea may also be supported by the fact that the absorption edge of ZrO_2/TaON undergoes a slight blue shift, compared to TaON (Figure 1 and Figure S7). The prevalent n-type photoresponse of the ZrO_2/TaON electrode can be explained by the idea that only a portion of the TaON surface undergoes such p-type modulation. This is reasonable, because the ZrO_2 modifiers were loaded on the TaON surface but did not completely coat the surface,[31] as also indicated by HR-TEM observations (Figure S2). Because the present ZrO_2/TaON is a polycrystalline powder, investigation of its detailed semiconducting character remains difficult but will be an important part of our future work.

In an n-type semiconductor photocatalyst, electrons tend to accumulate in the bulk while holes undergo localization on the surface, due to the band bending characteristics with respect to aqueous solution.[2d] Recombination between bulk electrons and surface holes would therefore be the dominant path in an n-type semiconductor photocatalyst suspended in an aqueous solution.[13e] In addition, intrinsic electrons existing in the bulk of an n-type semiconductor have a significant impact on charge recombination. Accordingly, moderation of the n-type semiconducting character of TaON is expected to suppress recombination, resulting in high photocatalytic performance. This idea is consistent with our recent study of a kinetic model of a photocatalytic water-splitting mechanism on $(Ga_{1-x}Zn_x)(N_{1-x}O_x)$ powder, which is an n-type semiconductor.[13e] In relation to the idea concerning p-type modulation mentioned above, one may also consider that the enhanced activity of the ZrO_2/TaON system is attributed to the built-in electric field (p/n junction) in the material, as proposed by Lee et al.[2a,11b] In this case, the internal p/n junction in a photocatalyst minimizes an energy wasteful electron−hole recombination, thereby enhancing both reduction and oxidation reactions occurring on the photocatalyst surface. However, this is not the case for ZrO_2/TaON, where only reduction behavior (H_2 evolution) is improved with a slight drop in O_2 evolution activity,[31] precluding the possibility of activity enhancement due to improved charge separation resulting from the built-in electric field. Thus, moderation of the n-type semiconducting character of TaON by the formation of a composite with ZrO_2 is therefore another possible reason for the high photocatalytic activity of ZrO_2/TaON. Because most (oxy)nitride photocatalysts are n-type semiconductors, it is expected that the photocatalytic activity of these (oxy)nitrides would be improved by employing a similar surface modification to moderate the n-type semiconducting character. This possibility is currently under investigation.

4. Conclusion

We attempted to construct photocatalytic water-splitting systems driven by two-step photoexcitation of two different semiconductor photocatalysts using a modified ZrO_2/TaON species (H_2 evolution photocatalyst) and various O_2 evolution photocatalysts with shuttle redox mediators. The primary requirement to achieve overall water splitting is to facilitate both the reduction of protons and the oxidation of electron-donating ions on ZrO_2/TaON, for which appropriate modification with metal cocatalysts and control of the reaction conditions are both essential. Among the combinations tested, Pt/ZrO_2/TaON, Pt/WO_3, and IO_3^-/I^- pairs were shown to be the most active components, because each photocatalyst efficiently promotes the forward reactions involving the redox couple (photooxidation of I^- on Pt/ZrO_2/TaON and photoreduction of IO_3^- on Pt/WO_3), minimizing undesirable backward reactions. Under optimal conditions, the apparent quantum yield at 420.5 nm reached 6.3%, which is a new benchmark for visible-light-driven Z-scheme water splitting using particulate photocatalysts. The high performance was due at least in part to the suppression of electron−hole recombination in ZrO_2/TaON, which results from the moderation of the n-type semiconducting character of TaON by the formation of a composite with ZrO_2. Although (oxy)nitrides may have been viewed as photocatalysts that possess relatively low activity for H_2 evolution in water splitting,[2b,62b] the results of the present study clearly demonstrate their high potential for water splitting after appropriate surface modification and refinement of reaction conditions.

Acknowledgment. This work was supported by the Research and Development in a New Interdisciplinary Field Based on Nanotechnology and Materials Science program of the Ministry of Education, Culture, Sports, Science and Technology (MEXT) of Japan, and The KAITEKI Institute, Inc.

Supporting Information Available: Schematic illustration of experimental setups for photocatalytic reactions (Figure S1), results of HR-TEM observation and EDS analysis for Pt/ZrO_2/TaON (Figure S2), time course of water formation in the dark over a mixture of Pt/ZrO_2/TaON and Pt/WO_3 suspended in an aqueous NaI solution (Figure S3), reproducibility test for AQY measurement (Figure S4), comparison of the activity of the ZrO_2/TaON-based system with that of the TaON-based system (Figure S5), time courses of H_2 evolution from aqueous NaI solution over Pt/ZrO_2/TaON with and without the addition of $NaIO_3$ (Figure S6), band-gap estimation for TaON and ZrO_2/TaON (Figure S7), and XRD patterns of TaON and ZrO_2/TaON (Figure S8). This material is available free of charge via the Internet at http://pubs.acs.org.

JA1009025

(64) Mishima, T.; Matsuda, M.; Miyake, M. *Appl. Catal. A: Gen.* **2007**, *324*, 77.